Journal of Visualization, Vol. 9, No. 1 (2006)91-99

Numerical Flow Visualization of a Single Expansion Ramp Nozzle with Hypersonic External Flow

Thiagarajan, V.*[1], Panneerselvam, S.*[1] and Rathakrishnan, E.*[2]

*1 Aerodynamics Division, Defence Research and Development Laboratory, Hyderabad, India.
*2 Department of Aerospace Engineering, Indian Institute of Technology, Kanpur, India.
E-mail: erath@iitk.ac.in

Received 21 March 2005
Revised 17 June 2005

Abstract : Numerical simulation of scramjet asymmetric nozzle flow is carried out to visualize and investigate the effects of interaction between engine exhaust and hypersonic external flow. The Single Expansion Ramp Nozzle (SERN) configuration studied here consists of flat ramp and a cowl with different combinations of ramp angle and cowl geometry. Using *PARAS 3D,* simulations are performed for a free stream Mach number of 6.5 that constitutes the external flow around the vehicle. Appropriate specific heats ratio has been simulated for the jet and free stream flow. External shock wave due to jet plume interaction with free stream flow, the internal barrel shock wave and the shear layer emanating from the cowl trailing edge and sidewalls are well captured. Wall static pressure distribution on the nozzle ramp for different nozzle expansion angles has been computed for both with and without side fence. Axial thrust and normal force have been evaluated by integrating the wall static pressure. Effect of cowl length variation and side fence on the SERN performance has also been studied and found to be quite significant. Based on this study, an optimum ramp angle at which the SERN generates maximum axial thrust is obtained. SERN angle of 20^{o} was found to be optimum when the flight axis coincides with nozzle axis.

Keywords : Hypersonic nozzle, SERN, Ramp nozzle, Hypersonic aftbody, Scramjet.

1. Introduction

Future high-speed air-breathing vehicles are subjected to extremely different flight and ambient conditions since the operating Mach number ranges are very wide. For such vehicles, the propulsive system will basically differ from the conventional concept. That is, integration of propulsion system with airframe components which is essential to meet the performance requirements. The propulsion-airframe integration task includes pre-compression of the incoming flow by vehicle forebody as well as expansion of combustion gas by thrust nozzle. The exhaust nozzle will encounter large variation in backpressure over the flight regime. Generally, these variations are handled with variable area nozzle that adjusts the exit area to the change in back pressure. For hypersonic vehicles with scramjet propulsion system, however, the operating nozzle pressure ratio i.e., the ratio of jet total pressure to ambient pressure is very high (Deere and Asbury, 1999). With conventional exhaust system, matching the nozzle exit pressure to the atmospheric condition to optimize thrust force is extremely difficult. Single Expansion Ramp Nozzle (SERN) integrated with the airframe is a viable solution to overcome these challenging requirements. Many countries are concentrating on the

research and development of hypersonic air-breathing vehicles since these vehicles have high potential in terms of their high speed, higher altitude of atmospheric flight operation and compactness for their application in civil, space and military sectors. However, there have been only a few reports on hypersonic nozzle performance that are unclassified (Spaid and Keener, 1995; Berens 1993). The external SERN surface has an asymmetric configuration due to having only upper solid surface. Lower region of the scramjet engine exhaust flow interacts with the hypersonic flow around the vehicle. Since the available thrust in the operational Mach number range of the scramjet engine is very small relative to the overall thrust, the nozzle performance must be accurately predicted, including the effect of the interaction of the exhaust and external flow. Though experiments are very valuable because of the quick information that they yield, it does not seem feasible to approach the problem systematically by experiments alone, because of large number of design parameters. The less expensive and faster numerical study may help to determine the sensitivity of the various parameter variations to select an optimized version of nozzle system. In the present study, 2D and 3D simulations are conducted on a straight SERN using *PARAS 3D* software. Analysis has been carried out for one nozzle entry condition with different ramp angles, cowl geometries and side fence. These results are discussed here.

2. Vehicle Configuration and Simulation Approach

An artistic view of a typical hypersonic vehicle configuration with highly integrated propulsion system is shown in Fig. 1. This vehicle is designed to operate in the free stream Mach number range of 4 to 6.5. The cruise Mach number is 6.5 and the corresponding altitude is 32.5 km. The details of mission analysis and aerodynamic configuration design are given in Panneerselvam et al. (2001). The propulsion system is a dual mode ramjet engine with an intake, an isolator, a combustor and SERN. The approach for the nozzle simulation illustrating the free stream flow and jet flow is presented in Fig. 2.

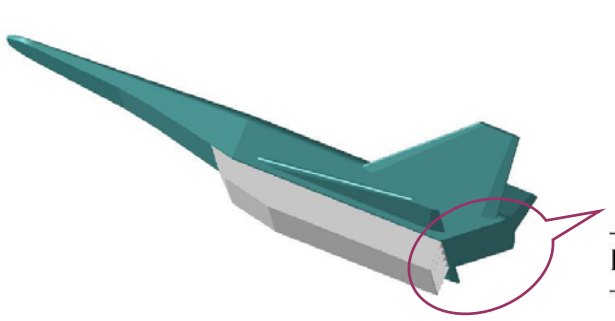

Fig. 1. Hypersonic air-breathing vehicle.

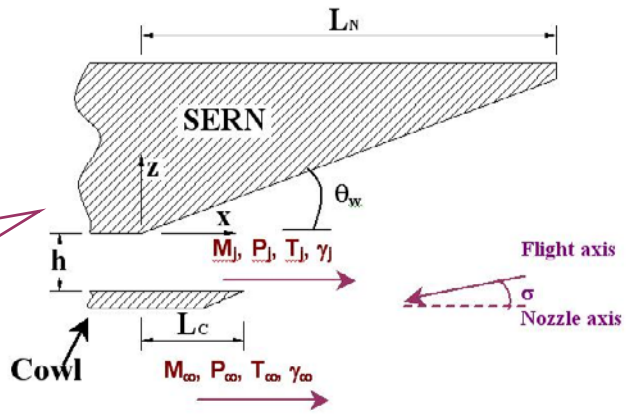

Fig. 2. Numerical simulation approach.

3. Computational Procedures

The computations in this study are performed with PARAS software, a three-dimensional, Navier-Stokes solver. Solution strategy of this code is to march in time in a local time stepping mode for faster convergence. The code can solve viscous flow using finite volume method on a Cartesian grid. The turbulent solver uses the two equations k-ε model to obtain the turbulent stresses. Wall damping effects of turbulent flow are considered by means of a modified wall function approach. More details of PARAS code are found in (User Manual, 2000). The surface grid generated for

computing the flow field is shown in Fig. 3.

The initial grid size for the 2D and 3D computations are 100 x 50 and 100 x 50 x 50 respectively. The grid around the body is generated by means of a rectangular adaptive Cartesian mesh technique. Cartesian cells used in the code are of three types, namely air cells, body cells and partial cells. The cells, which are partial and near partial are split, to further resolve the body shape. The grids get adapted automatically based on body geometry during grid generation and based on flow gradients during solution procedure. In flow or outflow, wall boundaries and reflection boundaries are the boundary conditions encountered in the present calculations. Conservative flow variables; pressure (P), temperature (T), Mach number (M), and specific heats ratio (γ) for both jet and free stream flow were frozen in the case of supersonic inflow boundary. At the outflow, the flow variables were extrapolated from the interior. Modified wall function was applied for wall boundary.

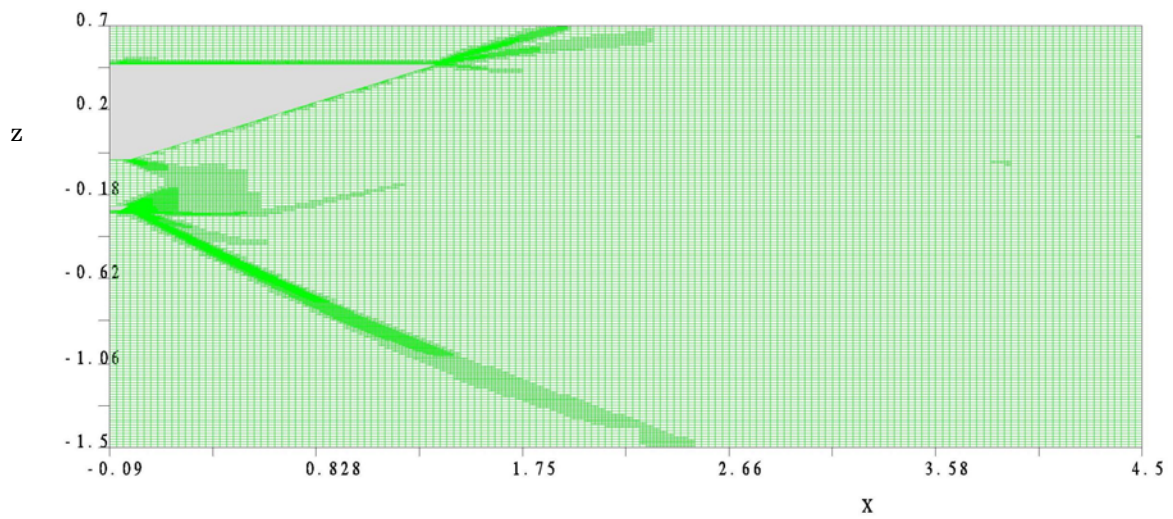

Fig. 3. Computational domain and the grid for SERN configuration (x-z plane).

4. Results and Discussion

4.1 NSAP SERN Configuration

Initially, National Aero Space Plane aftbody configuration (Spaid and Keener, 1995) was numerically simulated for the validation of the existing numerical code. The computation was performed for the nozzle with free stream flow and jet gas flow as air. The nozzle conditions at which the computations carried out are presented in Table 1. The subscripts ∞, *j* and *t* represent the free stream, jet and total conditions, respectively. The computed wall pressure is compared with experimental data in Fig. 4. It is observed that the predictions compare very well with the measured data. With the confidence gained from the above exercise, the computational studies on a generic SERN configuration are performed. The jet and free stream values for the generic SERN computations are given in Table 2.

Table 1. NASP SERN entry and free stream conditions.

M_∞	M_j	P_{tj}/P_∞	$P_{t\infty}$	$T_{t\infty}$	P_{tj}	T_{tj}
7.33	1.74	310	6895 kPa	828 K	374 kPa	272 K

Table 2. Generic SERN entry and free stream conditions.

M_∞	M_j	P_j/P_∞	T_j/T_∞	γ_∞	γ_j
6.5	1.71	36	9.92	1.4	1.25

4.2 Nozzle Flow Filed and Wall Static Pressure

A series of two-dimensional and three-dimensional numerical tests were carried out to visualize and analyze the effects on nozzle performance due to the interaction between engine exhaust and hypersonic external flow. The 2-D results are discussed in this section.

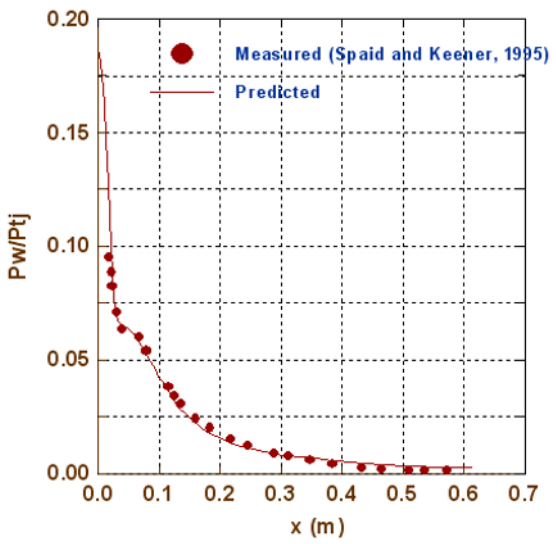

Fig. 4. Comparison of wall static pressure between computed and measured.

The predicted flow pattern due to the interaction of free stream flow with the jet flow is shown in Figs. 5 and 6. The iso-contour plots of density and Mach number is shown for the nozzle ramp angle of 20°. Three distinct features are noticed from the flow patterns; an external shock, internal barrel shock and shear layer. The interaction of the outward turning jet with external flow causes the jet plume external shock wave. In addition to the external shockwave, an internal shock wave in the jet originates near the nozzle cowl trailing edge. In between the shocks, a jet shear layer is observed, which is formed by the difference in velocity between the jet and external flow. A shear layer emanates from the cowl trailing edge as a thin layer and its thickness increases along the downstream direction. These features are more clearly seen in the constant density contour plot.

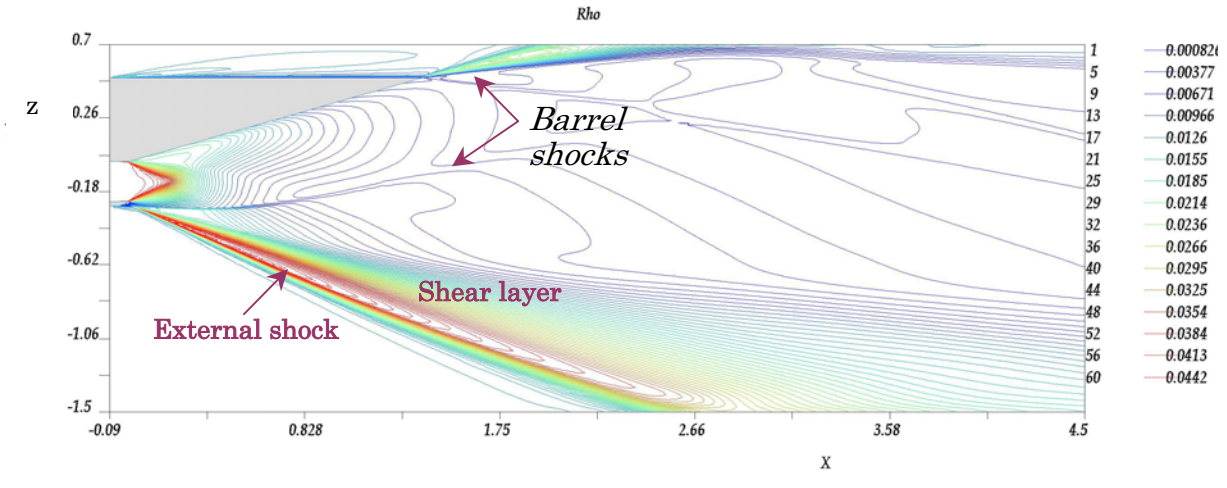

Fig. 5. Predicted constant density contour.

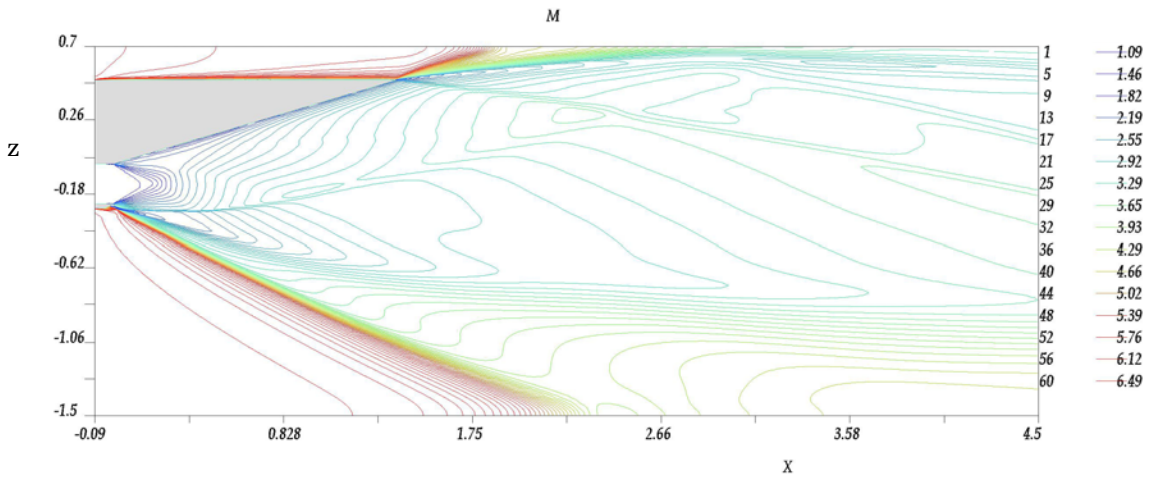

Fig. 6. Predicted constant Mach number contour.

The computed wall static pressure distribution along the nozzle of a generic SERN configuration for different ramp angles (θ_W = 15° to 35° in steps of 5°) are shown in Fig. 7. For all the ramp angles, after a sharp reduction in the static pressure near the expansion corner of the ramp, the pressure distribution is nearly constant for a distance and then decreases asymptotically along the nozzle. A simple Prandtl-Meyer expansion is taking place near the nozzle entry. The influence of expansion fans from the cowl lip on the ramp is felt only at a distance downstream from the nozzle entry. This distance of constant pressure region varies approximately from 1.2h to 2h as the ramp angles increases from 15° to 35°. Where h is the nozzle entry height (m).

4.3 Nozzle Force Characteristics

The nozzle efficiency or the ability to convert the momentum at its entrance into useful thrust is mainly a function of its geometries viz., expansion angle, length, cowl length, etc. In order to determine the optimum nozzle angle, which influences the axial thrust, the nozzle with constant entry conditions is examined first. Here the cowl length and the nozzle exit to entrance area ratio are held constant. Only the nozzle ramp angle and ramp length are varied. The axial thrust and normal force are evaluated by integrating the SERN wall pressure distribution. In general, the thrust vector lies in the plane of nozzle axis for conventional rocket nozzles. However, the highly integrated scramjet nozzle has large asymmetric force components normal to the nozzle axis. As a result of variation in flight path angle and wall radii/angularity on the ramp surface, the nozzle force vectors do not lie normal to nozzle wall inclination angle and hence the thrust axis is inclined to nozzle axis. Since the thrust in the flight direction determines the vehicle acceleration characteristics, the angle between the flight axis and nozzle axis (σ) has to be considered in the nozzle design. The value of σ equal to zero implies that the flight axis and nozzle axis lies in the same plane.

The variation of axial thrust coefficient ($C_T = T_h/qS_{ref}$) with respect to L_N/h for different σ is shown in Fig. 8. Here L_N – nozzle length (m), T_h – thrust (N), q – dynamic pressure (N/m^2) and S_{ref} – reference area (m^2). From the point of view of maximum axial thrust, the nozzle with ramp angle of 20° is found to be optimum when σ = 0. As σ increases to 4 and 8°, the ramp angle at which maximum axial thrust generated is increases to 25° with lesser C_T.

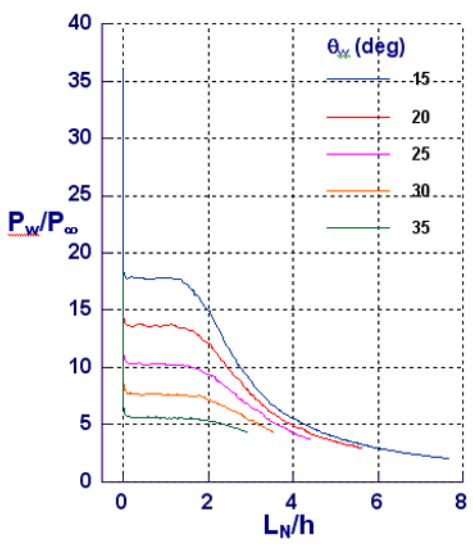

Fig. 7. Static pressure distribution on the nozzle wall (y = 0).

4.4 Effect of Nozzle Cowl Length

The length of the nozzle cowl (L_C) is extended downstream by a distance $0.5h$ and $1h$ to study the effect on the nozzle performance. For each L_C/h, computations were performed with different θ_W. The predicted nozzle force characteristics for three cowl configurations are compared in Fig. 9.

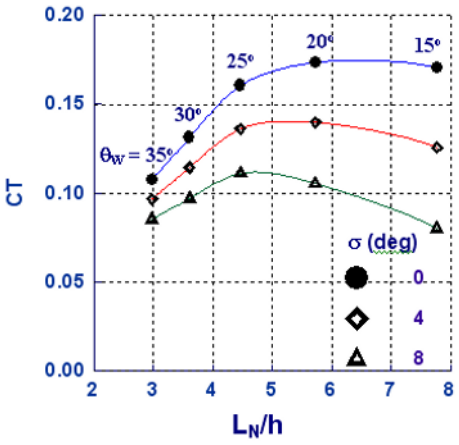

Fig. 8. Nozzle force characteristics.

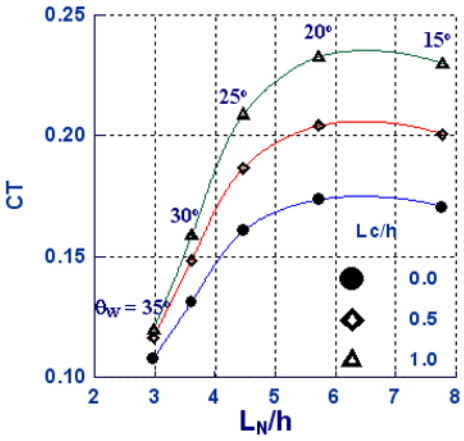

Fig. 9. Effect of nozzle cowl length.

Extension of nozzle cowl has a beneficial effect on nozzle thrust. In the case of 20° nozzle ramp angle, which corresponds to L_N/h of 6.87, the thrust coefficient is increased by 17% and 32% when the cowl is extended to $0.5h$ and $1.0h$ respectively. At higher ramp angles, i.e., ramp angle beyond 25°, the increase in thrust coefficient due to cowl extension is found to be negligible.

5. Effect of Side Fence

3D simulations were performed on SERN with ramp angle 20°. Nozzle entry and free stream flow conditions are same as given in Table 2. The performance of the nozzle has been studied with and without side fence. The sectional view of 3-D SERN and the forces acting on the nozzle are illustrated in Fig. 10. Side fence was introduced for the entire nozzle length. The height of side fence at the nozzle entry and exit are h and 0.2h respectively. Width of the nozzle is constant and w/h is 1.92.

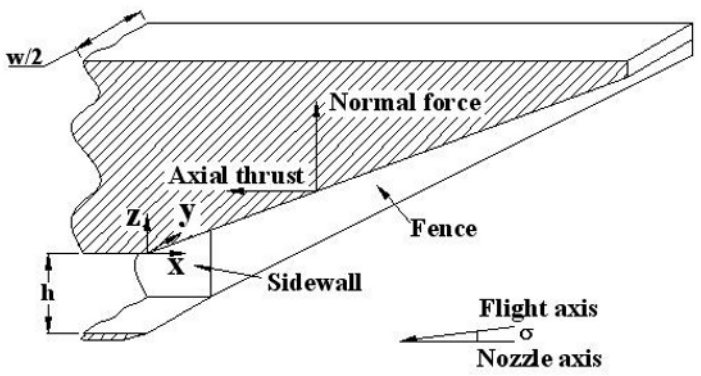

Fig. 10. Sectional view of 3-D nozzle.

For nozzle without side fence, the computed flow field in the symmetry plane at three axial stations is shown in Fig. 11. These iso-contour plots of density shown in x-z plane are for the half model of the nozzle and corresponding ramp angle is 20°. Flow features as noticed in the case of 2D flow are seen here also. In addition to these, it is observed that the streamlines are drifting outwards due to large pressure difference between the jet exhaust and external flow i.e., the flow expands three dimensionally outward from the center of the jet plume. The shear layer nearly fills the region between the internal and external plume shock, but these features become more widely separated in the down stream. Near the ramp edge, the shear layer merges with corner flow.

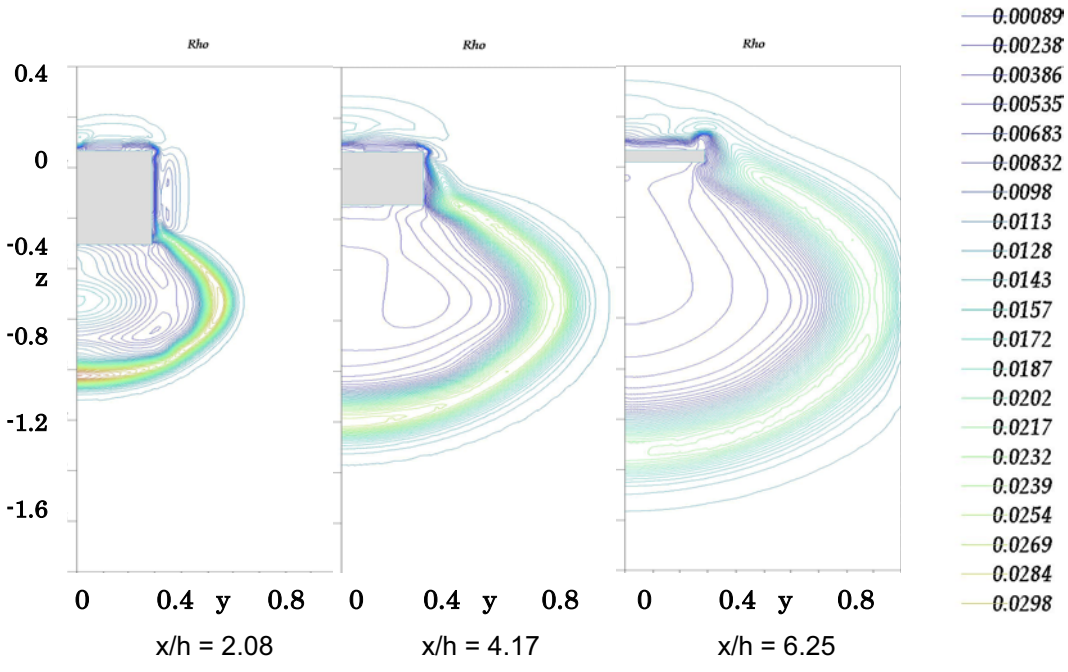

Fig. 11. Predicted constant density contour plots at different axial station (Without side fence; ramp angle = 20°).

Figure 12 shows the corresponding transverse cross-section views of the flow field with side fence. With the side fence, the streamlines between the fences do not drift outwards as noticed in the case of without side fence. The wall static pressure distributions computed at different spanwise stations on the nozzle surface are shown in Fig. 13 for both without and with side fence. In the case without side fence, the results show that the jet flow does not expand smoothly on the ramp surface but separates because of the influence of the internal shock within the jet fence (Fig. 13a)). It is

believed that this cross-flow separation on the ramp surface is induced by the interaction of the wall boundary layer with the intercepting shock from the sidewall trailing edge. With side fence, the pressure distribution is almost two-dimensional and the spanwise pressure variation is much small compared that without side fence (Fig. 13b)), leading to greater nozzle thrust. Cross flow separation observed in the case without side fence was not detected with side fence.

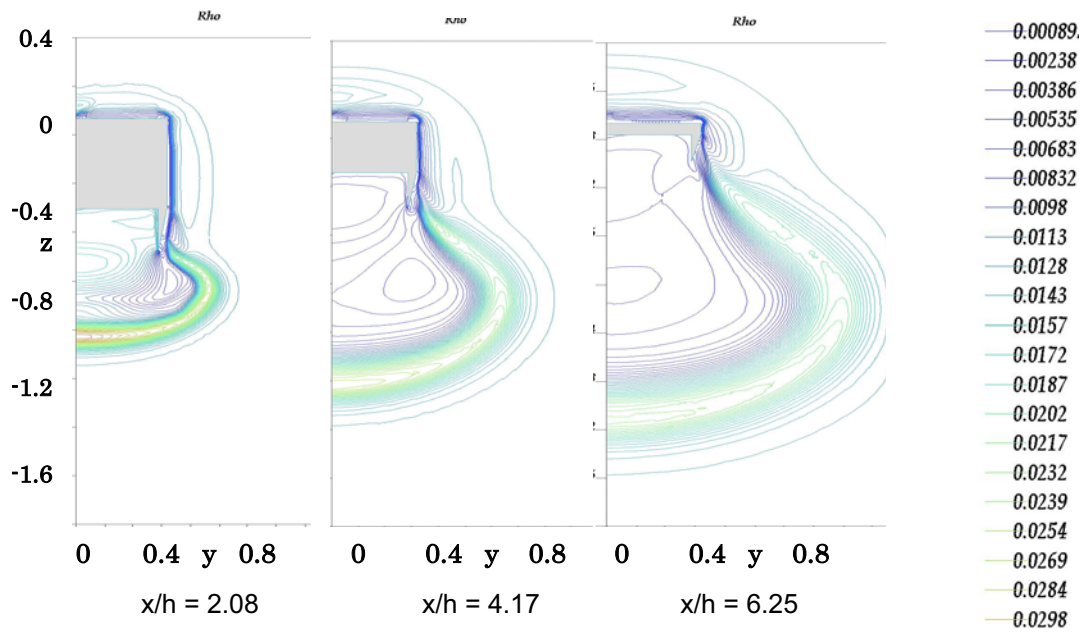

Fig. 12. Predicted constant density contour plots at different axial station (With side fence; ramp angle = 20°).

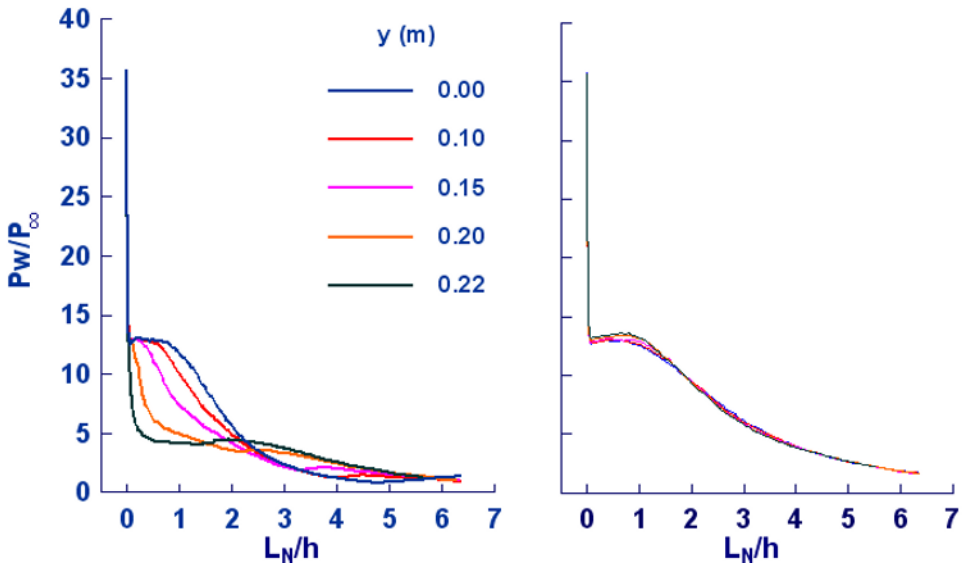

a) Without side fence b) With side fence

Fig. 13. Pressure distribution on the ramp at different spanwise stations.

6. Conclusions

Simulation has been carried out on a straight SERN configuration using *PARAS 3D* software. External shock wave due to jet plume interaction with free stream flow, the internal barrel shock wave and the shear layer emanating from the cowl trailing edge and sidewalls are well captured. The results show that, angle between the flight axis and the nozzle axis is an important design parameter, which influences the nozzle thrust greatly. From the point of view of maximum axial thrust, the nozzle with ramp angle of 20^o was found to be optimum when the flight axis lies with the nozzle axis. Extension of nozzle cowl has a beneficial effect on nozzle thrust. Thrust coefficient increment of 17% and 32% were obtained when the cowl is extended from 0 to $0.5h$ and $1.0h$ respectively. The increase in thrust coefficient due to cowl extension at higher ramp angles is found to be negligible. 3D results shows that cross-flow separation of the exhaust flow is apparent in the ramp side region. In the presence of side fence, nozzle flow becomes almost two-dimensional and improves the nozzle performance in terms of axial thrust. This study forms a high fidelity database, which can be used as a basis for the formal optimization technique such as response surface methodology.

References

Berens, T., Numerical Investigation of Thrust Vectoring by Injection of Secondary Air into Nozzle Flows, AGARD Meeting on Computational and Experimental Assessments of Jets in Cross Flows, (1993-4).

Deere, K. A. and Asbury, S. C., Experimental and Computational Investigation of a Translating Throat, Single-Expansion-Ramp Nozzle, NASA TP 209138, (1999).

Panneerselvam, S., Ganesh Anavaradham, T. K., Geetha, J. J. and Thiagarajan, V., Review Document of Conceptual Design of Hypersonic Research Vehicle, No. DRDL. 5120.1004.000, (2001-12).

Spaid, F. W. and Keener, E. R., Experimental Results for Hypersonic Nozzle/Afterbody Flow Field, NASA TM 4638, (1995,3).

User Manual for PARAS 3D, VSSC/TT/81/00, (2000-11).

Author Profile

Thiagarajan, V.: He received his B.Tech degree from Madras Institute of Technology, Chennai, India in 1990 and M.E. degree in Aerospace Engineering from Indian Institute of Science, Bangalore, India in 1992. His research interests are air-intake and nozzle aerodynamics for hypersonic air-breathing vehicle. He is currently pursuing his Ph.D degree at Indian Institute of Technology, Kanpur, India.

Panneerselvam, S.: He received his Ph.D degree from Indian Institute of Technology Madras, Chennai. He has contributed tremendously to the design and development of Indian guided missile programme. His research areas include missile aerodynamics, design and development of hypersonic air-breathing vehicle. Currently he is the Technology Director, Aerodynamics at Defence Research and Development Laboratory, Hyderabad, India.

Rathakrishnan, E.: He received his Ph.D degree from Indian Institute of Technology Madras, Chennai and currently is a professor of Aerospace Engineering at Indian Institute of Technology, Kanpur, India. He is well known internationally for his research in the area of jets, base flows and drag reduction. He is a fellow of Royal Aeronautical Society.